Voltage-induced bending and electromechanical coupling in lipid bilayers

Ben Harland,[1,2] William E. Brownell,[3] Alexander A. Spector,[1,2] and Sean X. Sun[1,3,4]
[1]*Department of Mechanical Engineering, The Johns Hopkins University, Baltimore, Maryland 21218, USA*
[2]*Department of Biomedical Engineering and The Whitaker Institute of Biomedical Engineering, The Johns Hopkins University, Baltimore, Maryland 21218, USA*
[3]*Department of Chemical and Biomolecular Engineering, The Johns Hopkins University, Baltimore, Maryland 21218, USA*
[4]*Department of Otolaryngology-Head and Neck Surgery, Baylor College of Medicine, Houston, Texas 77030, USA*
(Received 2 December 2009; revised manuscript received 19 January 2010; published 9 March 2010)

The electrical properties of the cellular membrane are important for ion transport across cells and electrophysiology. Plasma membranes also resist bending and stretching, and mechanical properties of the membrane influence cell shape and forces in membrane tethers pulled from cells. There exists a coupling between the electrical and mechanical properties of the membrane. Previous work has shown that applied voltages can induce forces and movements in the lipid bilayer. We present a theory that computes membrane bending deformations and forces as the applied voltage is changed. We discover that electromechanical coupling in lipid bilayers depends on the voltage-dependent adsorption of ions into the region occupied by the phospholipid head groups. A simple model of counter-ion absorption is investigated. We show that electromechanical coupling can be measured using membrane tethers and we use our model to predict the membrane tether tension as a function of applied voltage. We also discuss how electromechanical coupling in membranes may influence transmembrane protein function.

DOI: 10.1103/PhysRevE.81.031907 PACS number(s): 87.16.dm, 46.70.Hg, 82.45.Mp

I. INTRODUCTION

In living organisms, large electric fields are mostly absent, except in the vicinity of the cell membrane where the electric potential may change by hundreds of millivolts over a distance of 4–6 nm. Experimental evidence suggests that a particular electromechanical coupling occurs naturally in lipid bilayers: the so-called flexoelectric effect [1,2]. This phenomenon is an analog of the electromechanical behavior of piezoelectric crystals. In addition to changing linear dimension, lipid bilayers also undergo curvature changes as voltages are applied. Two kinds of flexoelectricity are typically discussed: The direct flexoelectric effect describes changes in the membrane polarization resulting from changes in curvature. The converse flexoelectric effect describes spontaneous changes in curvature which occur in response to applied electric fields. In this paper, we relate the molecular level charge distributions in the lipid bilayer to measurable macroscopic mechanical properties using a theoretical model. The model predicts that voltage and curvature-related ion adsorption at the bilayer-solvent interface is the essential physical process that gives rise to flexoelectricity. Predictions of the theory can be checked experimentally by measuring the tensile forces in lipid tethers attached to voltage-clamped cells [3–5].

The coupling of voltages to interfacial surface tensions has been a topic of investigation since the experiments of Lippmann [6,7]. Flexoelectricity in lipid bilayers was first experimentally observed in the 1970s when AC currents were detected in membranes subjected to mechanical oscillations (direct effect) [8]. Since then, increasingly reliable measurements have been obtained for the converse effect. Experiments have measured oscillations of bilayer patches subjected to AC voltages [9] and atomic force microscope (AFM) tip deflections have been used to quantify the effect in a whole cell voltage-clamp setup [10,11].

The traditional description of flexoelectricity is phenomonelogical; curvature and voltage are related through the *flexocoefficients* [12,13]. To date, theoretical models have been limited to the direct effect [14], the electrostatic contribution to the bending modulus [15–18], and conformational instabilities in the presence of applied electric fields [19]. To our knowledge, no previous work has addressed voltage-driven bilayer bending and this is the main goal of this paper. We present a molecular-scale model of charge interaction to address electromechanical coupling and the flexoelectric effect. The model used is based on a density functional approach, utilizing the Marcus model of charge solvation in a dielectric medium [20,21]. We compute the bending energetics of the membrane subjected to an applied voltage. Absorption of ions into the bilayer surface is addressed through the inclusion of a molecular potential corresponding to the phospholipid chemical environment. This may be regarded as an extension of the Gouy-Chapman approach (e.g., see [22]). Alternative models such as the Langmuir adsorption isotherm are also discussed, but we find that the alternative models give qualitatively similar results and represent a quantitative change only. The results of the model can be assessed experimentally in simple cylindrical geometries such as in a membrane tether. The influence of electromechanical coupling on membrane protein function is also addressed.

II. ELECTROMECHANICAL MODEL OF THE LIPID BILAYER

The theoretical approach is to consider the lipid bilayer as a spatially inhomogeneous dielectric decorated with solvated

charge distributions. Our model bilayer consists of symmetric leaflets containing a mixture of anionic (25%) and zwitterionic (75%) phospholipid molecules. The surplus negative charge is balanced by positive counterions, which reside both within the region occupied by the phospholipid headgroups as well as the neighboring electric double layers.

The total free energy of a lipid bilayer can be formally written as a sum of electrical and mechanical contributions,

$$F = F_{el} + F_m. \tag{1}$$

The exact forms of these free-energy functionals are not known. A number of models have been developed to describe membrane mechanics [23–25]. The Helfrich model describes the membrane as an elastic surface connected to a lipid reservoir, and uses 2 mechanical constants, κ and γ to describe bending and stretching deformations, respectively [23],

$$F_m = \int dA\left(\frac{1}{2}\kappa c^2 + \gamma\right). \tag{2}$$

The integral is over the bilayer surface and c is the total curvature (for geometries considered in this work, Gaussian curvature is either zero or an invariant and is neglected). Writing the free energy in the form of Eq. (1), the constants κ and γ will describe the mechanical contributions only, as if the membrane does not have charges.

The electrostatic free energy, F_{el}, determines the equilibrium charge configuration of the membrane. More precisely, the electrostatic free energy function should determine two fields: the polarization (dipole field) in the medium, $\mathbf{p}(\mathbf{x})$, and the distribution of charges in the medium $\rho(\mathbf{x})$. We regard the bilayer as a set of continuous charge distributions in a varying dielectric medium. The details of these charges are described in Fig. 1. The charges are of three types: bilayer charges of the phospholipid headgroups, ρ_0, positive ions which have adsorbed into the bilayer surface, n_+, and external ionic charges, $\rho_{\text{ions}} = en_+ - en_-$. The total charge distribution is then

$$\rho(\mathbf{x}) = \rho_0(\mathbf{x}) + en_+(\mathbf{x}) - en_-(\mathbf{x}), \tag{3}$$

of which we assume ρ_0 is fixed to the bilayer medium and $n_\pm$ are allowed vary. Note that n_+ ranges from the "interior" of the bilayer into the medium, but n_- only exist in the medium. This is because there is a favorable binding interaction between ρ_0 and n_+ (see below), but unfavorable interaction between ρ_0 and n_-.

The electrostatic free energy of these charges can be modeled using the Marcus theory of polarizable media [20,21]. In this model, F_{el} is a functional of $n_+(\mathbf{x})$, $n_-(\mathbf{x})$ and $\mathbf{p}(\mathbf{x})$, and is composed of several parts.

$$F_{el} = E_c + E_p + E_v - TS, \tag{4}$$

E_c is the Coulomb energy,

$$E_c = \frac{1}{2}\int d\mathbf{x}\rho(\mathbf{x})\psi_0(\mathbf{x}), \tag{5}$$

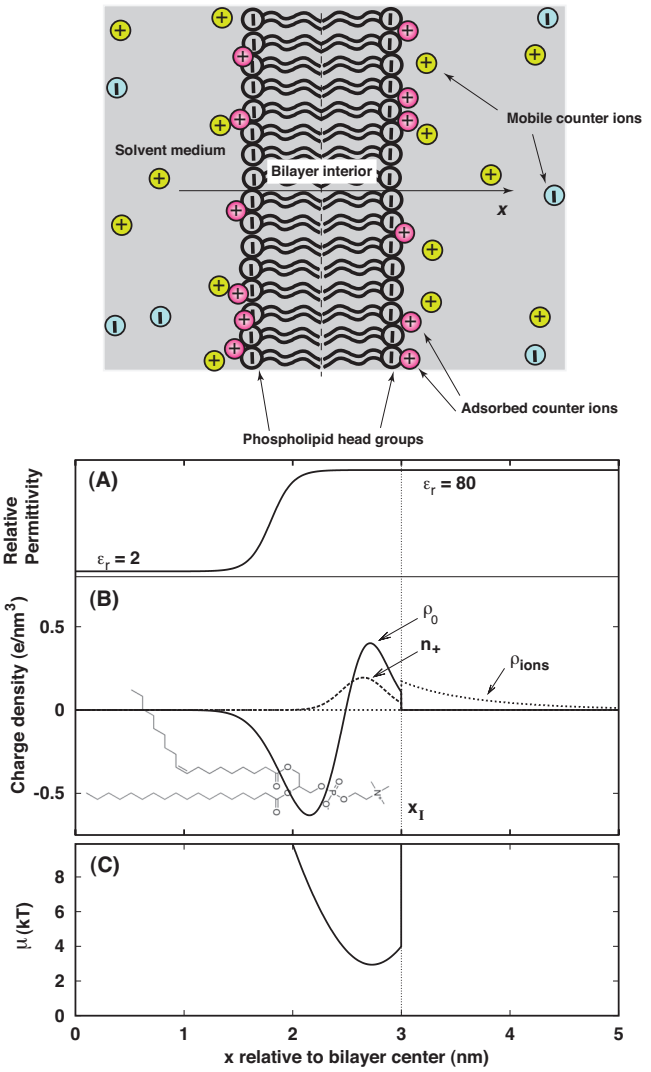

FIG. 1. (Color) Charge distributions in a flat bilayer. We consider a model bilayer which is a mixture of 75% zwitterionic phospholipid (phosphaditylcholine) and 25% anionic phospholipid (phosphatidylserine). The surrounding aqueous medium is a 150 mM 1:1 electrolyte. (a) The relative permittivity of the medium. (b) Charge densities used in the model. The intrinsic charges for the bilayer, ρ_0 are from [26–28]. These correspond to the molecular structure of the phospholipid molecules. Additionally, mobile bilayer charges, n_+, represent adsorbed counterions. These are dynamic and allowed to respond to voltages. The densities integrate so that the overall charge per unit area for each leaflet is -0.02 C/m^2 at vanishing potential difference ($+0.06$ C/m^2 for the combined positive charges and -0.08 C/m^2 for the negative charges.) (c) The molecular field, $\mu(x)$ in Eq. (23), is used to compute the amount of adsorbed charges at the surface of the bilayer as the applied voltage is changed.

where ρ is the total charge density, and ψ_0 is the electrostatic potential from ρ in a vacuum:

$$\psi_0(\mathbf{x}) = \int d\mathbf{x}' \frac{\rho(\mathbf{x}')}{|\mathbf{x} - \mathbf{x}'|}. \tag{6}$$

The excess polarization energy is

$$E_p = \frac{1}{2}\int d\mathbf{x}\frac{4\pi}{\epsilon(\mathbf{x})-1}\mathbf{p}^2(\mathbf{x}) + \frac{1}{2}\int d\mathbf{x}\int d\mathbf{x}'\frac{\nabla\cdot\mathbf{p}(\mathbf{x})\nabla'\cdot\mathbf{p}(\mathbf{x}')}{|\mathbf{x}-\mathbf{x}'|} - \int d\mathbf{x}\nabla\cdot\mathbf{p}(\mathbf{x})\psi_0(\mathbf{x}) \tag{7}$$

where $\epsilon(\mathbf{x})$ is the dielectric constant and $\mathbf{p}$ is the polarization.

The Marcus theory assumes that charges only interact with each other through the polarizable medium. At the lipid-solvent interface, however, the phospholipid head groups also chemically bind with the positive mobile ions. Therefore, there should be another term that accounts for the chemical energy of n_+ binding to the phospholipid headgroups through an interaction potential, V,

$$E_v = \int d\mathbf{x}\int d\mathbf{x}' n_+(\mathbf{x})V(\mathbf{x},\mathbf{x}')\rho_0(\mathbf{x}') \tag{8}$$

The functional form of V is not known, but we may write

$$E_v \to \int d\mathbf{x} n_+(\mathbf{x})\mu(\mathbf{x}) \tag{9}$$

with

$$\mu(\mathbf{x}) = \int d\mathbf{x}'\rho_0(\mathbf{x}')V(\mathbf{x},\mathbf{x}'). \tag{10}$$

Specific values for μ may be fit to charge distributions obtained from molecular simulations performed under zero-voltage conditions (see the bottom panel of Fig. 1) [26–28]. We assume that $\mu(\mathbf{x})$ is independent of bilayer curvature and applied voltage. These assumptions are unlikely to be correct and are made due to the lack of available data.

The entropy component of the free-energy functional treats the mobile ions as solutes in an ideal solvent,

$$-TS = k_B T\sum_{i=\pm}\int d\mathbf{x} n_i(\mathbf{x})\left(\ln\frac{n_i(\mathbf{x})}{n_0} - 1\right) \tag{11}$$

where n_0 is the bulk ion concentration. In principal, there should also be an entropy contribution from the lipid charges ρ_0, however, this is neglected since these charges are "fixed" to the bilayer, and the density changes during bending do not lead to any appreciable changes in the entropic free energy.

Equation (4) is the precursor to the constitutive equations of electrostatics after variations with respect to $\mathbf{p}(\mathbf{x})$, $n_+(\mathbf{x})$, and $n_-(\mathbf{x})$. These coupled equations are

$$\frac{\delta F_{el}}{\delta\mathbf{p}(\mathbf{x})} = 0, \tag{12}$$

$$\frac{\delta F_{el}}{\delta n_+(\mathbf{x})} = 0, \tag{13}$$

$$\frac{\delta F_{el}}{\delta n_-(\mathbf{x})} = 0. \tag{14}$$

Equation (12) leads to the following equation for the equilibrium polarization:

$$\frac{4\pi}{\epsilon(\mathbf{x})-1}\mathbf{p}(\mathbf{x}) + \nabla\psi_0 - \nabla\int d\mathbf{x}'\frac{\nabla'\cdot\mathbf{p}(\mathbf{x}')}{|\mathbf{x}-\mathbf{x}'|} = 0, \tag{15}$$

which can be rewritten as

$$\mathbf{p}(\mathbf{x}) = \frac{\epsilon(\mathbf{x})-1}{4\pi}\mathbf{E}(\mathbf{x}), \tag{16}$$

from which the definition of the electrostatic field emerges,

$$\mathbf{E}(\mathbf{x}) = -\nabla\psi_0(\mathbf{x}) + \nabla\int d\mathbf{x}'\frac{\nabla'\cdot\mathbf{p}(\mathbf{x}')}{|\mathbf{x}-\mathbf{x}'|}. \tag{17}$$

Since the electric displacement is defined as $\mathbf{D}(\mathbf{x})=\mathbf{E}(\mathbf{x})+4\pi\mathbf{p}(\mathbf{x})$, we also recover the correct constitutive relation of electrostatics. Since the electric displacement satisfies $\nabla\cdot\mathbf{D}(\mathbf{x})=4\pi\rho(\mathbf{x})$, the minimized polarization field satisfies the Poisson equation:

$$\nabla\cdot\epsilon(\mathbf{x})\mathbf{E}(\mathbf{x}) = -\nabla\cdot\epsilon(\mathbf{x})\nabla\psi(\mathbf{x}) = 4\pi\rho(\mathbf{x}), \tag{18}$$

where $\psi(\mathbf{x})$ is the total electrostatic potential, and is related to the minimum polarization by

$$\psi(\mathbf{x}) = \psi_0(\mathbf{x}) - \int d\mathbf{x}'\frac{\nabla'\cdot\mathbf{p}(\mathbf{x}')}{|\mathbf{x}-\mathbf{x}'|}. \tag{19}$$

In practice, it is equivalent to solve the Poisson equation of Eq. (18) or solve the self consistent Eq. (15). In our calculations, we solve Eq. (18) to find ψ, $\mathbf{E}$ and the equilibrium $\mathbf{p}$. Once $\mathbf{p}$ is found, the electrostatic energy terms simplify and become

$$E_c + E_p = \frac{1}{2}\int d\mathbf{x}\rho(\mathbf{x})\psi_0(\mathbf{x}) + \frac{1}{2}\int d\mathbf{x}\mathbf{p}(\mathbf{x})\cdot\nabla\psi_0(\mathbf{x}). \tag{20}$$

It may also be shown that the variation of the minimized electrostatic energy with respect to the charge distribution is

$$\frac{\delta(E_c+E_p+E_v)}{\delta\rho(\mathbf{x})} = \psi(\mathbf{x}). \tag{21}$$

In the solvent region, Eq. (14) gives

$$k_B T\ln\left[\frac{n_-(\mathbf{x})}{n_0}\right] - e\psi(\mathbf{x}) = 0 \tag{22}$$

which is the usual Boltzmann distribution for the negative mobile charges: $n_-(\mathbf{x})=n_0 e^{\beta e\psi(\mathbf{x})}$. Similarly, Eq. (13) yields the distribution

$$n_+(\mathbf{x}) = n_0 e^{-\beta[e\psi(\mathbf{x})+\mu(\mathbf{x})]}. \tag{23}$$

In the solvent, $\mu\to 0$ and the ions satisfy the Poisson-Boltzmann Equation. Within the bilayer, the positive ions may respond to changes in their electrostatic environment. The model used here is mean field throughout and, therefore, neglects ion correlations. Adsorption of finite-sized ions onto a surface can be alternatively treated using an Ising-like

model, with the population of adsorbed ion determined by the Langmuir Isotherm [29],

$$n_+(\mathbf{x}) = \frac{n_0}{1 + Ke^{\beta e(\psi(\mathbf{x}_l) - \psi_b)}}. \tag{24}$$

Here, K is a constant that is chosen to obtain the desired charge adsorption concentration at zero voltage and ψ_b is the potential in the bulk. We found the results from both of these approaches to be qualitatively the same, with a reduction in the magnitude of electromechanical coupling of around 30% when using Eq. (24) rather than Eq. (23).

The modeling approach here allows us to compute the free energy of a bilayer system as a function of the applied voltage and the geometry of lipid charge distributions. For instance, if the bilayer is bent, ρ_0 in the inner and outer leaflet compress and expand leading to a change in the overall free energy. Thus, by investigating the electrostatic free energy as a function of bilayer curvature c and the applied voltage V_0, we can predict the electrostatic contributions to electromechanical coupling. This paper considers simple geometries, but complicated charge distributions can be investigated in the same way.

Our computational scheme is to solve the constitutive equations self-consistently. A shooting procedure is employed to integrate Eqs. (18), (22), and (23) subject to the boundary conditions $\lim_{\mathbf{x}\to\pm\infty} \nabla\psi = 0$. Integration is carried out using the second order Taylor formula. In cylindrical coordinates this is

$$\psi_{i+1} = \psi_i + dr\psi_i' + \frac{dr^2}{2}\left(\psi_i'' + \frac{1}{r_i}\psi_i'\right), \tag{25}$$

where ψ_i is the value of the potential at position r_i and dr is the grid spacing. The derivatives ψ_i' and ψ_i'' are obtained through Gauss' Law and the Poisson Equation, respectively.

$$\psi_i' = -\frac{1}{\epsilon_i}\frac{Q_i}{A_i}, \tag{26}$$

$$\psi_i'' = -\frac{1}{\epsilon_i}(\rho_i + \epsilon_i'\psi_i') - \frac{1}{r_i}\psi_i, \tag{27}$$

The charge density, ρ_i, is given by the total charge density in Eq. (3). Q_i is total charge enclosed by a cylindrical surface with radius r_i and surface area A_i. The shooting procedure is performed in two stages. First, integration is carried out in a forward direction from the center of the bilayer, where the correct value of ψ is sought which gives the correct outer boundary condition, $\lim_{r\to\infty} \psi(r) = 0$. Next, shooting is performed in reverse from this value, this time the search being for the correct value of V_0 which is consistent with $\lim_{r\to 0} \psi(r) = V_0$ and $\psi'(0) = 0$.

The electrostatic potential difference arises due to a charge imbalance between the two leaflets of the bilayer. The bilayer as a whole is neutral and this charge imbalance, which is imposed experimentally through the voltage-clamp apparatus, is localized to the immediate vicinity of each bilayer-solvent interface [30,31]. Computationally, the charge imbalance is specified by the integrated charge of the inner leaflet and it's associated electrolyte. A search for the particular quantity of this charge is carried out in order to produce the desired potential difference. The value of $\lim_{\mathbf{x}\to+\infty} \psi(r)$ is taken to be zero and the potential difference is denoted V_0. Representative solutions are shown in Fig. 2.

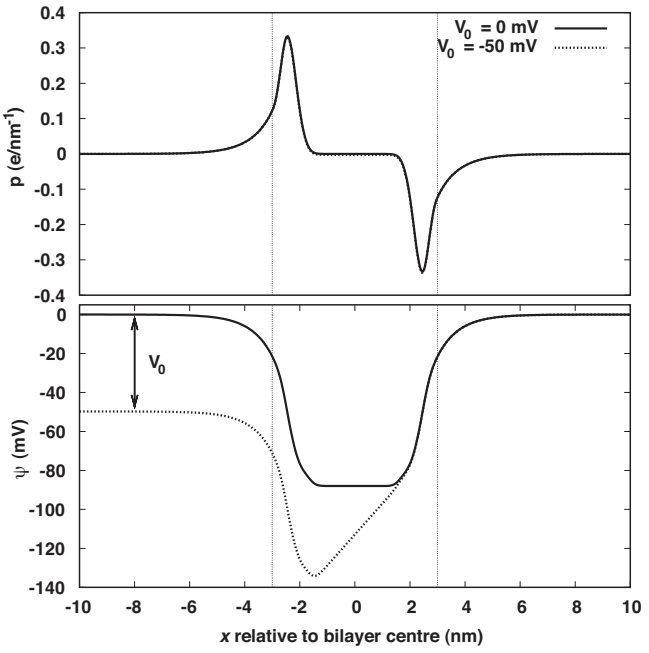

FIG. 2. The solution from the Poisson Boltzmann equations for the electrostatic potential (bottom panel) and the corresponding polarization density (top panel) for flat bilayers with $V_0 = 0, -50$ mV.

III. RESULTS

A. Flexoelectricity and the electrostatics of bilayer bending

To examine flexoelectricity, we must relate the free energy of our bilayer system to the applied voltage, V_0, and curvature, c. We consider cylindrically shaped bilayers only, so there is a single curvature $c = 1/R$, where R is the radius of curvature, measured from the center of the cylinder to the center of the bilayer. We compute the electrostatic component of the free-energy per unit area of bending for the (cylindrically shaped) bilayer system, $\Delta f_{el} = \Delta F_{el}/A$. This is given by the free energy difference between the flat and curved case with V_0 held fixed,

$$\Delta f_{el}(c, V_0) = f_{el}(c, V_0) - f_{el}(0, V_0), \tag{28}$$

where the subscript *el* refers to the component of the overall free energy that is strictly electrostatic.

We consider a bilayer, in which there is no lipid exchange between the inner and outer leaflet. (In cells, lipid exchange between the inner and outer leaflet is catalyzed by flippases which operate on the time scale of tens of minutes [32]). As curvature is introduced, the fixed charges in the inner leaflet are compressed and charges on the outer leaflet are expanded,

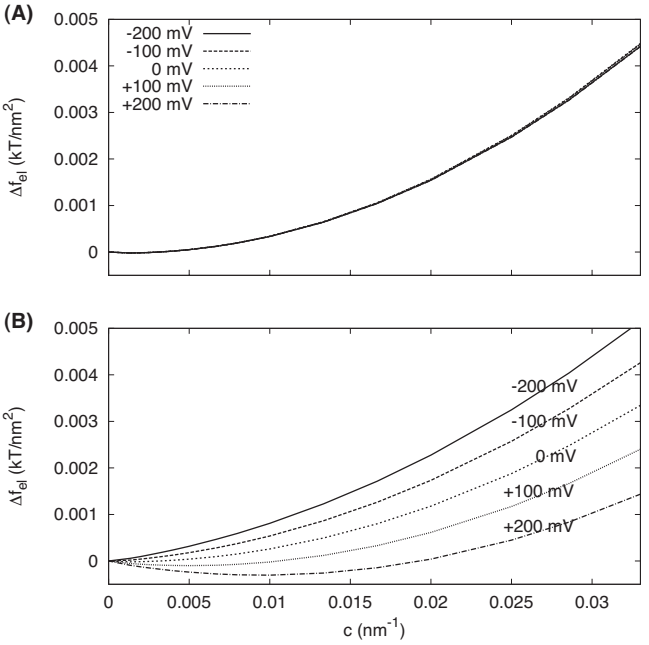

FIG. 3. The computed electrostatic free energy change per unit area for bilayer bending ($\Delta f_{el}=[F_{el}(R,V_0)-F_{el}(R=\infty,V_0)]/A$) with different values of V_0. The x-axis is the curvature of the membrane cylinder, $1/R$. Different models for the adsorbed charges are shown: (a) Fixed n_+ in the bilayer region; (b) Molecular field model. Both models show an electrostatic contribution. However, only (b) shows a voltage dependence, indicating that a dynamic adsorbed charge layer is required for flexoelectricity. In (b), for some voltages, the free energy change is negative, suggesting that voltages make curvature generation favorable.

$$\rho_0(r;R)=\rho_0(r;R\to\infty)\times\frac{R}{r}, \tag{29}$$

where r is the coordinate perpendicular to the membrane.

Results for Δf_{el} are shown in Fig. 3. For comparison, results are also shown in which dynamic ion adsorption is neglected (fixed n_+ in the bilayer region); the voltage dependence of these curves is found to be critically dependent on this adsorption.

It is interesting to first consider the curves in Figs. 3(a) and 3(b), which correspond to zero applied voltage (or more accurately, where the voltage is clamped at 0 mV). The electrostatic energy in this case increases quadratically with bilayer curvature, i.e., there is an electrostatic contribution to the bending modulus. This contribution is significant: nonlinear least-squares fits (to $\Delta f_{el}=\frac{1}{2}\kappa_{el}c^2$) provide an estimate for the bending modulus of $\kappa_{el}=10\ k_BT$ in Fig. 3(a) and $\kappa_{el}=6\ k_BT$ in Fig. 3(b). These values may be compared to an experiment [33] which estimated this electrostatic contribution to the bending modulus to be $3-5\ k_BT$ for dimyristoylphosphatidylcholine vessicles. For comparison, a typical value for the overall bending modulus of a bilayer is $\sim 20\ k_BT$.

Subtracting the $V_0=0$ mV curve gives the component of bending free energy which is strictly voltage dependent, which we shall call Δf_V. The results (shown in Fig. 4) suggest the following functional form:

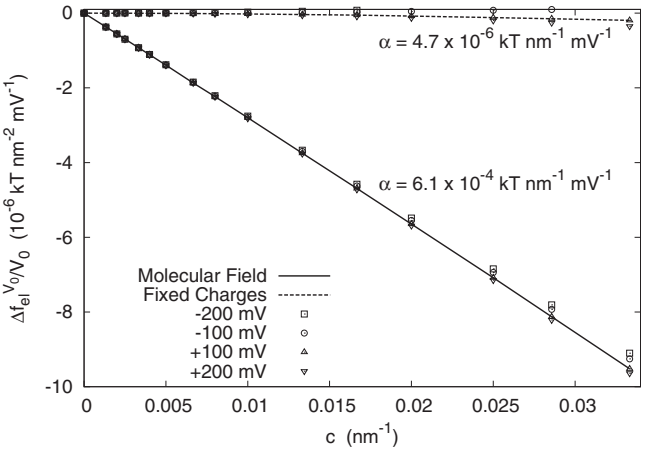

FIG. 4. The computed voltage-dependent bending free energy density per mV as a function of curvature (symbols). This plot is obtained by subtracting the $V_0=0$ mV curve from Fig. 3 and dividing by the voltage. The lines are the theoretical fit of Eq. (30). This plot is used to justify the form of Eq. (31).

$$\Delta f_V(c,V_0)=-\alpha V_0 c, \tag{30}$$

where α is an electromechanical coupling constant. It makes sense to partition the total free energy of Eq. (1) into a part that describes $V_0=0$ and a part that describes the dependence on the voltage,

$$\Delta f(c,V_0)=\Delta f_0(c)+\Delta f_V(c,V_0)=\left(\frac{1}{2}\kappa c^2+\gamma\right)-\alpha V_0 c. \tag{31}$$

This functional form is in agreement with the expression of Glassinger and Raphael [34] which used a phenomenological electromechanical coupling coefficient. Here, we see that the microscopic model is able to compute the coupling coefficient α. Moreover, although we do not assume a linear model from the onset, evidently the model predicts a bilinear coupling term between voltage and curvature.

1. Direct flexoelectric effect

The direct flexoelectric effect describes the generation of an electric potential difference across a membrane as a result of deformation [1]. The relationship is phenomonologically linear, and in the case of a cylindrically shaped bilayer can be expressed,

$$V_0=\frac{f}{\epsilon_0}c. \tag{32}$$

The proportionality constant, f, is called the *direct flexocoefficient*. In this situation, voltages develop in the absence of any charge separation across the membrane. The results from our model are shown in Fig. 5.

Experimental measurements for the flexocoefficient have been made on a variety of membranes and suggest a range of $\pm(0.1-100)e$ [35] although a few units of electric charge are typical. Estimates provided by our model are 0.025 e for the

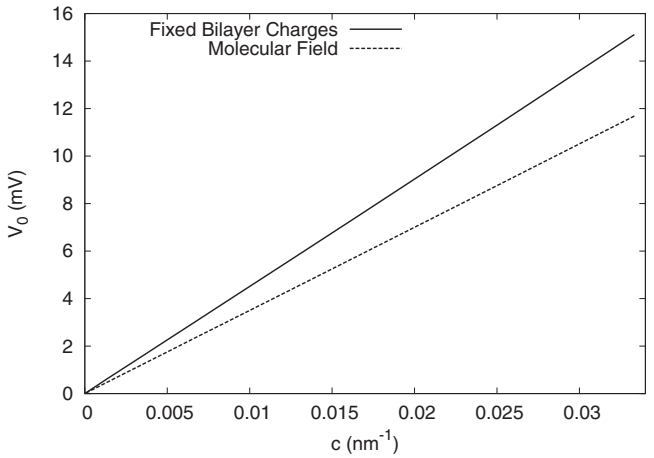

FIG. 5. The computed relationship between the bilayer curvature, c, and voltage, V_0, is linear. The flexoelectric coefficient, f, can be estimated from the slope of these curves. The direct flexoelectric effect exists even when lipid charges are fixed.

case where bilayer charges are fixed and 0.019 e when bilayer charges are computed using Eq. (22). It is observed that when bilayer charges are permitted to rearrange, they will do so in order to reduce curvature induced voltages and, therefore, the system free energy.

Analytical expressions for f have been worked out in [14] by solving the linearized Poisson-Boltzmann Equation for a bilayer described by two charged plates (their theory does not take into account any local charge imbalance across the bilayer). Adsorption of charges was included using a Langmuir isotherm. Their results do not significantly differ from ours, although direct comparison would require that we map our charge distributions onto delta functions located at the bilayer surface. If we choose these surfaces to be separated by 5.6 nm, their formulas provide flexocoefficients, which are in perfect agreement with ours.

It is worth commenting that a common definition of the direct flexoelectric effect relates curvatures to the electric polarization of the bilayer, a reference to the original liquid crystal flexoelectricity proposed by Meyer [36],

$$P_s = fc, \tag{33}$$

$$= \frac{1}{R}\int drrp(r), \tag{34}$$

where $p(r)$ is the polarization shown in Fig. 2. We find that this definition leads to flexocoefficients which are an order of magnitude larger and of opposite sign than those obtained using Eq. (32). This sign change occurs because the medium in the vicinity of the inner leaflet, although more polarized, occupies a smaller volume than that of the outer leaflet. Thus, the integrated polarization density and the electric potential difference carry opposite orientation.

2. Converse flexoelectric effect

The manifestation of flexoelectricity, which is reciprocal to the direct effect is called the converse flexoelectric effect. This describes curvatures which are induced by applied electric fields according to the phenomonological relationship [1],

$$c_{\min} = \left(\frac{f}{\kappa}\right)E. \tag{35}$$

Here, $c_{\min}$ is the equilibrium curvature that minimizes the total free energy. The constant f is the *converse flexocoefficient*, κ is the elastic bending modulus, and E is the electric field, which will be assumed to be uniform within the bilayer, $E=V_0/h$, when making estimates for f. According to our model,

$$c_{\min} = \frac{\alpha}{\kappa}V_0, \tag{36}$$

so that we may write

$$f = \alpha h, \tag{37}$$

which for our model ($\alpha=0.0159\ e/\mathrm{nm}$) gives an estimate of $f=0.095\ e$.

3. Moment of bilayer bending

The interactions between lipid bilayers and mechanosensitive membrane channels has been the subject of experiments and simulations studies [37–39]. Lipid molecules exert a pressure on membrane proteins; these pressures are expressed as a lateral pressure profile. When an external voltage is applied, an additional pressure which is antisymmetrical will appear and the bilayer will undergo a deformation until this asymmetry is dissipated and the membrane will attain an equilibrium curvature.

We consider a flat bilayer of thickness h, in which the pressure is written in terms of two components,

$$p(z,V_0) = p_0(z) + \Delta p(z,V_0), \tag{38}$$

where z is the coordinate perpendicular to the bilayer surface ($z=0$ is taken to be the bilayer midplane). p_0 is the intrinsic membrane pressure profile in absence of voltages and Δp is the voltage-dependent component. We shall assume that the voltage-dependent pressure is proportional to the distance from the midplane, $\Delta p(z,V_0)=\lambda(V_0)z$. The amount of work performed by Δp on the bilayer to generate curvature dc can be written

$$dw = \int_{-h/2}^{+h/2} \Delta p(z,V_0)zdzdc = -\lambda(V_0)\frac{2}{3}\left(\frac{h}{2}\right)^3 dc. \tag{39}$$

Therefore the moment of bilayer bending can be related to the electromechanical coupling constant, α of Eq. (30),

$$\left.\frac{\partial w}{\partial c}\right|_{c=0} = -\lambda(V_0)\frac{h^3}{12} = -\alpha V_0, \tag{40}$$

$$\lambda(V_0) = \frac{12}{h^3}\alpha V_0. \tag{41}$$

The magnitude of Δp will be largest at the bilayer surface ($z=\pm h/2$), where

TABLE I. The magnitude of the maximum voltage-induced pressure within a bilayer over a range of transmembrane potentials. Our models predict that pressures from flexoelectric response of the membrane are too small to make a significant contribution to voltage response of transmembrane proteins.

V_0 (mV)	$\lvert\Delta p^{\max}\rvert$ (10^{-3} pN/nm^2)
0	0.00
±100	1.15
±200	2.29

$$|\Delta p_{\max}| = \frac{6}{h^2}\alpha V_0. \tag{42}$$

These pressures, shown in Table I, are small. Therefore, our model indicates that flexoelectricity does not appreciably contribute to the voltage sensitivity of ion channels or other membrane proteins.

B. Electromechanical forces in membrane tether experiments

Predictions of the flexoelectric properties of membranes can be obtained from membrane tether experiments using a setup depicted in Fig. 6 [40]. A large vesicle or a cell is voltage clamped such that the interior has a fixed potential, V_0. A tether is then pulled from it with an optical tweezer and the voltage-dependent tensile force experienced by the tether is recorded. This experiment is a sensitive test of electromechanical coupling in bilayers.

An estimate for these voltage-dependent tensile forces can be obtained within the framework of our model. For simplicity, we neglect any complex geometries of the bilayer occurring at the boundaries of the tether near the vesicle body; for long tethers, these geometries do not contribute to the tether tension [41]. We consider forces from a pure cylindrical bilayer membrane tether. In a real cell, however, other structures such as the cytoskeletal cortex and transmembrane proteins will change the mechanical properties of the membrane. Furthermore, the phospholipid composition of the inner and outer leaflet is not symmetric and transmembrane proteins will also effectively change the charge distributions of Fig. 1. Therefore, quantitative predictions of cellular results requires more experimental information. Nevertheless, the basic framework to explain the results remains the same.

For a membrane tether of length L and radius R, the tensile force is the derivative of the total free energy with respect to the tether length: $\tau = -\partial F/\partial L$. Using Eq. (31), this force is

$$\tau = -\frac{2\pi}{c}\left[\frac{1}{2}\kappa c^2 + \gamma - \alpha V_0 c\right] \tag{43}$$

where κ is the bending modulus and γ is the surface tension of the membrane. For typical membrane with mechanical parameters of $\kappa = 20\ k_BT$ and $\gamma = 0.05\ k_BT/\text{nm}^2$ [42,43], τ is on the order of 10 pN. There is also a contribution from in-plane deformation of the bilayer in response to the voltage. Such deformations are a consequence of the Maxwell stress tensor [44,45] and will introduce a voltage-dependence to the γ parameter. However, calculations from our model show that this contribution is small when compared to the out-of-plane electromechanical coupling and are neglected here. The equilibrium radius of the tether is obtained by minimizing Eq. (43) with respect to curvature,

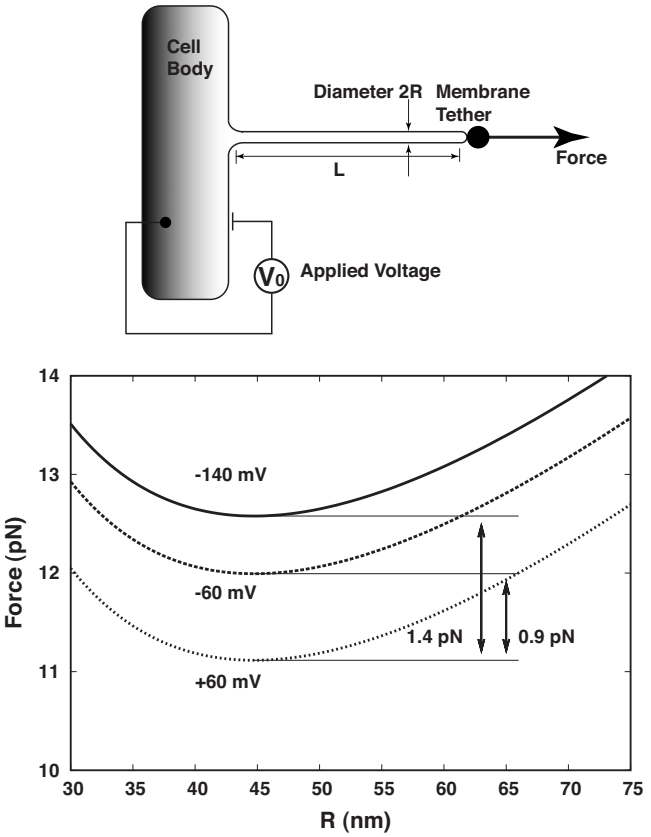

FIG. 6. The experimental setup. A cylindrical tether is drawn from a vesicle by a bead in an optical trap. The radius of tether is obtained by minimizing the overall free energy with respect to the tether radius. As the voltage is changed, the tensile force in the tether will change. Lower panel illustrates the optical trap force, $-\tau$ in Eq. (45), as a function of both voltage and the radius of the tether.

$$R_{\min} = c_{\min}^{-1} = \sqrt{\frac{\kappa}{2\gamma}}, \tag{44}$$

which gives the following expression for the observed tether force,

$$\tau = -2\pi(\sqrt{2\kappa\gamma} - \alpha V_0). \tag{45}$$

Although the absolute value of this force depends the choice for the parameters κ and γ, the changes in recorded tension as a cell or vesicle undergoes a voltage cycle depends only upon α. The linear relationship between voltage and tension is observed in experiments, the amount that the recorded tension changes per mV of clamped voltage is referred to as the *electromechanical gain* [3,46], which coincides with our term $2\pi\alpha$. Comparing the model predictions with experi-

TABLE II. Electromechanical gain, τ/V_0, predicted by our model with various treatments for ion adsorption. Presented for comparison are some experimental results obtained from cell membrane tethers.

Model	EM gain (pN/mV)
Fixed Bilayer Charges	0.0001
Langmuir Isotherm	0.007
Molecular Field	0.016
Experiment	
HEK cell[a]	0.026
Outer Hair cell[b]	0.3

[a]Reference [40].
[b]Reference [46].

mental measurements obtained from tethers attached to human embryonic kidney cells (Table II) shows agreement to within an order of magnitude. Because the electromechanical behavior of membrane tethers in real cells will be governed by a number of factors beyond the charge distributions within the bilayer, future experiments with vesicles where the lipid composition is controlled can further establish the validity of our model.

IV. DISCUSSION AND CONCLUSION

In this paper, we developed a molecular-level theory to understand the physical principles underlying the flexoelectric effect. We ask, to what extent can a simple mean-field electrostatic description account for experimental observations? The results are obtained by considering the curvature and voltage contribution to the free energy. We have shown that our continuum model for an isotropic and homogeneous charged lipid bilayer does exhibit compelling flexoelectric behavior, although the results suggest flexoelectric coefficients, which are small compared to experimentally observed values.

It is, however, not entirely clear how reliable the experimental estimates are. Dynamic oscillations of membranes, for example, are governed by not just the flexoelectric effect, but also viscoelasticity and a time-dependent surface tension, making results difficult to assess quantitatively. Observing AFM tips impinging on immobilized cells likewise requires that the surface tension contributing to the tip displacements be estimated through the Lippman equation [11]. Measurements of tensile forces in membrane tethers offers a simple and experimentally realizable method of obtaining accurate estimates for flexocoefficients in a static equilibrium regime. However, these measurements are performed on cells where membrane composition and the effects of transmembrane proteins are not controlled. It is desirable to have a set of measurements where lipid composition, ionic conditions and membrane tension are known, and a direct comparison between our model and experimental data would then be enlightening. Cellular membranes include proteins whose conformational changes and interaction with the membrane may result in in-plane voltage-dependent deformations. Thus, cellular membranes subjected to electric fields probably exhibit a three-dimensional response that combines out-of-plane (flexoelectric) and in-plane (piezoelectric) modes.

Of the variables in our model, the dynamic voltage-dependent nature of the adsorbed positive charges has the most marked effect on our results. This raises interesting questions about how ion adsorption is affected by both voltages and phospholipid densities. A notable simplification in our model is that changes in the chemical environment associated with increasing curvatures, beyond electrostatics, does not influence adsorption. Further simulation studies are needed to fully investigate the validity of our model and the nature of voltage coupled ionic dynamics at the lipid surfaces. The present model also assumes a rather simple geometry for the bilayer; more complex models that include thickness variations may introduce interesting effects as well.

Also, the importance of the distribution of charges at the bilayer surface suggests other interesting quantities to be investigated. The inclusion of multivalent ions, for example, or the intercalation of charged amino acid side chains with the phospholipid headgroups may be significant in determining membrane mechanical properties in response to voltages. Voltage-induced penetration of water, which, as a neutral dipole couples more weakly to electric fields than do ions, has been suggested in a mechanism for the electrical disruption of cell membranes [47]. The inhomogeneity of bilayer composition is another feature beyond the scope of the model presented here which is likely of importance. For example, the sequestering of cardiolipin in the bilayers of mitochondrial cristae has been implicated in the spontaneous and reversible formation of narrow tubular structures in response to changes in pH [48]. The relationship between pH and the electrical and mechanical properties of bilayers was the subject of another recent paper [49].

For the outer hair cell (OHC), the membrane protein prestin has been identified as a principal component of the motor complex that converts membrane voltages into active forces (e.g., [50]). There are a number of electromechanical models of prestin performance, in one proposed mechanism, prestin contributes to a dipole moment that drives the flexoelectric changes in the surrounding membrane [51]. In any case, the interaction of prestin with the applied electric field (electric charge transfer), is critical to the motor performance [52]. The theoretical framework presented here is useful for describing the ionic and electrostatic environment near prestin as well as other membrane proteins when voltages are applied. Our results also indicate that the voltage-dependent variations in the lateral pressure profile in the bilayer are quite small. Proteins such as voltage-gated channels probably do not experience significant forces from electromechanical coupling in the membrane.

The apparent importance of the flexoelectric paradigm for electromechanical coupling is not only of interest from a physiological point of view. It also has relevance to chemical biosensing in engineering applications [2]. Our work here lays out the theoretical foundations of this phenomenon and makes a connection of the molecular composition of the membrane; we also point out that further experimental inves-

tigations of the effect can be done using membrane tethers. Direct verification of many of the predictions of the model is possible with currently available optical tweezer technologies, computer simulations, and would shed light on the assumptions in the model.

ACKNOWLEDGMENTS

This work has been supported by research grants (Grant No. R01 DC000354) from NIDCD (NIH) and NSF (Grant No. CHE-0547041).

[1] A. G. Petrov, Curr. Top. Membr. **58**, 121 (2007).
[2] A. G. Petrov, in *Functionalized Nanoscale Materials, Devices and Systems*, edited by A. Vasaeshta and I. N. Mihailescu (Springer, Dordrecht, 2008), pp. 87–100.
[3] F. Qian, S. Ermilov, D. Murdock, W. E. Brownell, and B. Anvari, Rev. Sci. Instrum. **75**, 2937 (2004).
[4] F. Qian, S. Ermilov, D. Murdock, W. E. Brownell, and B. Anvari, Proc. SPIE **5331**, 112 (2004).
[5] R. Zhang, F. Qian, L. Rajagopalan, W. E. Brownell, and B. Anvari, Biophys. J. **93**, L07 (2007).
[6] M. G. Lippmann, Ann. Chim. Phys. **5**, 494 (1875).
[7] J. O. M. Bockris and A. K. N. Reddy, *Modern Electrochemistry: An Introduction to an Interdisciplinary Area* (Plenum, New York, 1973).
[8] A. L. Ochs and R. M. Burton, Biophys. J. **14**, 473 (1974).
[9] A. T. Todorov, A. G. Petrov, and J. H. Fendler, J. Phys. Chem. **98**, 3076 (1994).
[10] J. Mosbacher, M. Langer, J. Horber, and F. Sachs, J. Gen. Physiol. **111**, 65 (1998).
[11] P.-C. Zhang, A. M. Keleshian, and F. Sachs, Nature (London) **413**, 428 (2001).
[12] A. G. Petrov, *Physical and Chemical Bases of Biological Information Transfer* (Plenum Press, New York, 1975), pp. 111–125.
[13] A. G. Petrov, *The Lyotropic States of Matter. Molecular Physics and Living Matter Physics* (Gordon & Breach, New York, 1999).
[14] K. Hristova, I. Bivas, A. G. Petrov, and A. Derzhanski, Mol. Cryst. Liq. Cryst. **200**, 71 (1991).
[15] T. Chou, M. V. Jaric, and E. D. Siggia, Biophys. J. **72**, 2042 (1997).
[16] S. Genet, R. Costalat, and J. Burger, Biophys. J. **81**, 2442 (2001).
[17] M. Winterhalter and W. Helfrich, J. Phys. Chem. **96**, 327 (1992).
[18] M. Winterhalter and W. Helfrich, J. Phys. Chem. **92**, 6865 (1988).
[19] A. Fogden, D. J. Mitchell, and B. W. Ninham, Langmuir **6**, 159 (1990).
[20] R. A. Marcus, J. Chem. Phys. **24**, 966 (1956).
[21] R. A. Marcus, J. Chem. Phys. **24**, 979 (1956).
[22] M. Langner and K. Kubica, Chem. Phys. Lipids **101**, 3 (1999).
[23] W. Helfrich, Z. Naturforsch. C **28**, 693 (1973).
[24] G. Brannigan and F. L. H. Brown, Biophys. J. **90**, 1501 (2006).
[25] P. Wiggins and R. Phillips, Biophys. J. **88**, 880 (2005).
[26] P. Mukhopadhyay, L. Monticelli, and P. Tieleman, Biophys. J. **86**, 1601 (2004).
[27] S. Pandit, D. Bostick, and M. Berkowitz, Biophys. J. **84**, 3743 (2003).
[28] S. Pandit and M. Berkowitz, Biophys. J. **82**, 1818 (2002).
[29] I. Langmuir, Phys. Rev. **8**, 149 (1916).
[30] B. Roux, Biophys. J. **73**, 2980 (1997).
[31] M. Grabe, H. Lecar, Y. N. Jan, and L. Y. Jan, Proc. Natl. Acad. Sci. U.S.A. **101**, 17640 (2004).
[32] J. C. M. Holthuis and T. P. Levine, Nat. Rev. Mol. Cell Biol. **6**, 209 (2005).
[33] A. C. Rowat, P. L. Hansen, and J. H. Ipsen, Europhys. Lett. **67**, 144 (2004).
[34] E. Glassinger, A. C. Lee, and R. M. Raphael, Phys. Rev. E **72**, 041926 (2005).
[35] A. G. Petrov, Biochim. Biophys. Acta **1561**, 1 (2001).
[36] R. B. Meyer, Phys. Rev. Lett. **22**, 918 (1969).
[37] E. Perozo, A. Kloda, D. M. Cortes, and B. Martinac, Nat. Struct. Biol. **9**, 696 (2002).
[38] J. Gullingsrud and K. Schulten, Biophys. J. **86**, 3496 (2004).
[39] J. Yoo and Q. Cui, Biophys. J. **97**, 2267 (2009).
[40] B. Anvari *et al.*, *Auditory Mechanisms* (World Scientific, New Jersey, 2006), pp. 270–276.
[41] I. Derényi, F. Julicher, and J. Prost, Phys. Rev. Lett. **88**, 238101 (2002).
[42] E. Evans and W. Rawicz, Phys. Rev. Lett. **64**, 2094 (1990).
[43] J. Dai and M. P. Sheetz, Biophys. J. **77**, 3363 (1999).
[44] J. A. Cohen, B. Gabriel, J. Teissie, and M. Winterhalter, in *Planar Lipid Bilayers and their Applications*, edited by H. T. Tien and A. Ottova (Elsevier, New York, 2003), p. 847.
[45] D. Needham and R. M. Hochmuth, Biophys. J. **55**, 1001 (1989).
[46] Z. Li, B. Anvari, M. Takashima, P. Brecht, J. H. Torres, and W. E. Brownell, Biophys. J. **82**, 1386 (2002).
[47] D. P. Tieleman, BMC Biochem. **5**, 10 (2004).
[48] N. Khalifat, N. Puff, S. Bonneau, J. B. Fournier, and M. I. Angelova, Biophys. J. **95**, 4924 (2008).
[49] Y. Zhou and R. M. Raphael, Biophys. J. **92**, 2451 (2007).
[50] A. A. Spector, N. Deo, K. Grosh, J. T. Ratnanather, and R. M. Raphael, J. Membr. Biol. **209**, 135 (2006).
[51] R. M. Raphael, A. S. Popel, and W. E. Brownell, Biophys. J. **78**, 2844 (2000).
[52] S. X. Sun, B. Farrell, M. S. Chana, G. Oster, W. E. Brownell, and A. A. Spector, J. Theor. Biol. **260**, 137 (2009).